Original Paper

Osmotic Response of Dorsal Root Ganglion Neurons Expressing Wild-Type and Mutant KCC3 Transporters

Bianca Flores   Eric Delpire

Department of Anesthesiology and Neuroscience Graduate Program, Vanderbilt University School of Medicine, Nashville, TN, USA

Key Words
K-Cl cotransport • Cell Volume regulation • Regulatory Volume Decrease • Dorsal Root Ganglion neurons • Peripheral neuropathy

Abstract
Background/Aims: Loss-of-Function (LOF) of the potassium chloride cotransporter 3 (KCC3) results in hereditary sensorimotor neuropathy with Agenesis of the Corpus Callosum (HSMN/ACC). Our KCC3 knockout mouse recapitulated axonal swelling and tissue vacuolization observed in autopsies of individuals with HSMN/ACC. We previously documented the first human case of a KCC3 gain-of-function (GOF) in which the patient also exhibited severe peripheral neuropathy. Furthermore, the GOF mouse model exhibited shrunken axons implicating the cotransporter in cell volume homeostasis. It is unclear how both KCC3 LOF and GOF lead to peripheral neuropathy. Thus, we sought to study differences in cell volume regulation of dorsal root ganglion neurons isolated from different mouse lines. ***Methods:*** Using wide-field microscopy, we measured calcein fluorescence intensity through pinhole measurements at the center of cells and compared cell swelling and cell volume regulation/recovery of wild-type, LOF, and GOF dorsal root ganglia neurons, as well as wild-type neurons treated with a KCC-specific inhibitor. ***Results:*** In contrast to control neurons that swell and volume regulate under a hypotonic challenge, neurons lacking KCC3 swell but fail to volume regulate. Similar data were observed in wild-type neurons treated with the KCC inhibitor. We also show that sensory neurons expressing a constitutively active KCC3 exhibited a blunted swelling phase compared to wild-type neurons, questioning the purely osmotic nature of the swelling phase. ***Conclusion:*** These findings demonstrate the integral role of KCC3 in cell volume homeostasis and support the idea that cell volume homeostasis is critical to the health of peripheral nerves.

© 2020 The Author(s). Published by
Cell Physiol Biochem Press GmbH&Co. KG

Eric Delpire, Ph.D.

Department of Anesthesiology, Vanderbilt University School of Medicine,
T-4202 Medical Center North, 1161 21st Avenue South, Nashville, TN 37232-2520 (USA)
Tel. +1-615-343-7409, E-Mail eric.delpire@vanderbilt.edu

Introduction

KCC3 loss of function is well established as the primary cause of Hereditary Sensorimotor Neuropathy with Agenesis of the Corpus Callosum (HSMN/ACC) found in a French Canadian population [1, 2]. Patients with HSMN/ACC exhibit severe sensory and motor deficits with edema in their extremities [3–5]. Mouse models of a LOF of KCC3 recapitulate the peripheral neuropathy phenotype, sharing similarities in tissue pathology [1, 6]. Electron micrographs of sciatic nerves of the mouse model displayed axonal swelling and degeneration [7]. Furthermore, tissue vacuolization has been observed in dorsal root ganglion of mice that target KCC3 deletion in parvalbumin positive neurons [8]. The aforementioned tissue pathology has also been observed in autopsies of individuals with HSMN/ACC from the French-Canadian population, where carriers of the truncation of KCC3 exist in about 1 of 20 individuals [1]. Due to KCC3's ability to extrude K^+ and Cl^- ions and water, the cotransporter is involved in cell volume maintenance and regulation [9]. Thus, we hypothesized that the phenotypes observed were linked to a disruption in cell volume regulation. The logic underlying this hypothesis is strengthened by the knowledge that KCC3 activity is enhanced under swelling conditions [10, 11]. Therefore, the cells' inability to lose K^+ and Cl^- could lead to cell swelling upon slight osmotic perturbations.

Patients with HMSN/ACC suffer not only from peripheral nerve deficits, but also exhibit severe cognitive disabilities and schizophrenia-like symptoms, indicating both peripheral and central origins. KCC3, a swelling-activated K-Cl cotransporter, participates in the efflux of K^+, Cl^-, and water from cells that are exposed to swelling under hypotonic conditions [12]. The loss of ions and water helps the cells return to their original volume, through a process known as regulatory volume decrease. It is unclear exactly how LOF of KCC3 results in severe sensory and locomotor deficits, [1, 6, 13, 14] except to say that complete absence of KCC3 in mice leads to axonal swelling and some degree of axonopathy in both central [6] and peripheral nervous systems [7, 15].

Interestingly, we also documented the case of a young boy who carried a gain of function (GOF) mutation in KCC3 that led to a constitutively active cotransporter. The patient exhibited severe sensory and motor neuropathy, but was cognitively normal [16]. The GOF was caused by the substitution of threonine residue at position 991 into an alanine. The T991A mutation also resulted in severe locomotor deficits and nerve damage in homozygous mice [16]. Residues T991 and T1048 are the most critical sites in the phospho-regulation and activation of KCC3 [11], as the transporter only becomes active upon dephosphorylation of those sites [17, 18].

It is unclear how LOF and GOF in KCC3 both result in peripheral nerve disease. Electron microscopy of the sciatic nerve of LOF mice revealed axonal swelling, whereas the same analysis in GOF mice revealed significant axonal shrinkage, in addition to some myelin defects [7, 19]. Thus, our working model considers that volume homeostasis is critical to peripheral nerve integrity and function.

Cell volume regulation studies were previously conducted comparing cell swelling in T991A and control fibroblasts. Surprisingly, almost no swelling was observed in response to hypotonic challenges in the mutant cells [16]. This is clearly an abnormal behavior as the swelling phase following a hypotonic shock is typically regarded as a rapid re-equilibration of water across the plasma membrane with little participation of ions, which are far less permeable. Fibroblasts adhere tightly to their substrate, as their main function is to synthesize and provide extracellular matrix forming connective tissues in animals. In addition, they are not an adequate cell model system to assess the role of neuronal KCC3 in maintaining/regulating cell volume. In this study, we take advantage of our KCC3 knockout (KO) and KCC3-T991A mouse models to address the role of KCC3 in cell volume regulation. We utilized a large, rounded, and barely adherent, primary cell type: the dorsal root ganglion (DRG) neuron. DRG neurons have their cell bodies located in dorsal root ganglia. They transmit sensory information from the periphery (e.g. muscles, skin) to the spinal cord and central nervous system.

In both HSMN/ACC patients and KCC3 knockout mice sensory perception is impaired. In parvalbumin (PV)-driven KCC3 knockout mice, DRGs demonstrate tissue vacuolization and degeneration. Currently, we hypothesize that KCC3 cotransporter expression in sensory neurons participates in the maintenance of cell volume. We show that control DRG neurons (DRG neurons that have native KCC3 expression) volume regulate. Comparatively, DRG neurons lacking KCC3 are no longer able to undergo regulatory volume decrease following hypotonic swelling. In addition, we show that when KCC3 is constitutively active (T991A GOF), the cells exhibit significantly reduced swelling compared to wild-type cells upon a hypotonic challenge. This observation not only solidifies the view that the cotransporter is important in the cell volume maintenance and regulation of sensory fibers but also questions the nature of the swelling phase of the cell that results from the osmotic challenge.

Materials and Methods

Reagents

Phosphate Buffered Saline (Sigma, P7059-1L), Calcein-AM (ThermoFisher Scientific, C1430), Boric Acid (Sigma Aldrich, 10043-35-3), NaCl (RPU, S23020-1000.0), Sodium tetraborate decahydrate (Fisher chemical, S246-500), Fisherbrand Microscope cover glass (12-545-CIR -1.5.), Matek 35 mm Dish, 14 mm glass diameter (P35G-1.5-14-C), Polyethylenimine (Sigma, P3143), Laminin mouse protein (Gibco, 23-017-015), Collagenase (Roche Diagnostics, 11088882001), Trypsin (Sigma, T-4665), DNase I (Roche Diagnostics, 10104159001), Trypsin Inhibitor (Sigma, T-9128), Tween 20 (Sigma, P7949), Triton x-100 (Sigma, T-8787), Dulbecco's Modified Eagle Medium Nutrient Mixture F-12 (Gibco, 11320-033).

Animals

All animal handling and experimental procedures were approved by Vanderbilt's Institutional Animal Care and Use Committee and done in accordance with guidelines provided by the National Institutes of Health. The KCC3 knockout and KCC3-T991A mouse lines were previously described by us [1, 16].

Coverslip preparation

Prior to plating the DRG neurons, coverglass slips were placed on 35-mm Matek glass bottom dishes. Glass coverslips were plated overnight with 1% Polyethylenimine (PEI) diluted in borate buffer (100 mM boric acid, 75 mM NaCl, and 25 mM Na-tetraborate) and incubated at 37°C, 5% CO_2. The next day, PEI was washed 3 times with autoclaved water. Laminin (30 μg/ml) was then placed on the glass coverslips and incubated overnight at 37°C, 5% CO_2. Laminin was aspirated prior to cell plating.

Dorsal Root Ganglion (DRG) extraction and cell culture

Adult mice were euthanized with isoflurane and immediately dissected to remove T1-L5 DRGs. As described in [20], the vertebrae column was extracted, placed on ice, and then cut in half, ventral side facing upwards to remove the spinal cord and extract the DRGs. Once removed, DRGs were placed in a T-25 flask containing complete culture media, and then transferred to culture media containing collagenase, DNAse I, and Trypsin. The flask was placed in a 37°C heated water bath and gently shaken for one hour. After incubation, the DRGs were vigorously shaken to disintegrate clumps and Trypsin inhibitor was added. The cells were then spun down at 900 rpm for 4 min, resuspended 200 μl of control media. Cells were plated at a concentration of 200,000 cells per coverslip, in 2 ml of culture media per plate. Neurons were cultured on the PEI and laminin coated coverslips. The neurons were left to incubate and settle for two hours at 37°C prior to adding additional complete media and were imaged approximately 24 hours later.

Saline Solutions

The isotonic solution contained 80 mM NaCl, 3 mM KCl, 1 mM $CaCl_2$, 1 mM $MgCl_2$, 5 mM glucose, and 10 mM HEPES, pH 7.4. The osmolarity was adjusted to 300 mOsM through the addition of 115 mM sucrose. Hypotonic (180, 240 mOsm) solutions were obtained by reducing the amount of sucrose, and hypertonic solutions (420, 345 mOsm) were adjusted with increasing concentrations of sucrose.

Cell volume measurements

We utilized the Nikon Multi Excitation Tirf in wide field mode to measure changes in fluorescent intensity. These changes in intensity are used as a proxy for cell volume as previously described [21, 22]. Fluorescence intensity was measured using Plan Apo VC 20x/0.75 magnification. DRG neurons were incubated with calcein-AM (0.03 μM) diluted in isotonic media for 25 minutes at 37°C and washed three times with isotonic media prior to placing the coverslip in the chamber. Calcein is a single excitation dye with a good signal to noise ratio [23]. Each glass coverslip of neurons was placed in an open-top chamber platform (Warner instruments P-1, 64-0277) in a perfusion chamber (RC-26GLP). Solutions were perfused by gravity columns to ensure even flow of changing solutions. Images were captured using an Andor Zyla sCMOS camera, a Lumencor Spectra X light engine (with filters) as the light source, and with the Perfect Focus System turned on to avoid focus drifting. Cells were continuously perfused and imaged every 15 seconds for 16 min (3 min in isotonic media, followed by a 10 min osmotic challenge, and a final return to isotonic media for 3 min). Calcein was excited at 470 nm and emission was collected at 525 nm ± 50 nm.

Changes in fluorescence intensity were measured using region of interest pinhole measurements placed in the middle of the cell, utilizing the Time Lapse imaging setting in NIS Elements. Background was subtracted from fluorescent intensity measurements. Note that in graphs denoting changes in volume, have their Y axis denoted FΔ/F0 (change in Fluorescence/Initial fluorescence).

The area of the cells was measured using NIS elements software region of interest area detection. Volume was then extrapolated from the measured area assuming a perfect sphere, as DRG keep a round shape under all osmolarities.

Immunostaining

DRG cell culture was prepared as aforementioned and allowed to sit for 24 hours before staining. Cells were briefly washed with Hank's Balanced Salt Solution, without calcium, nor magnesium. An ice cold 1:1 methanol acetone mixture was then added for cell culture fixation for 20 minutes. The fixation solution was removed and cells were treated with 5% BSA, 1% goat serum, 0.5% Tween 20, 0.5% Triton X-100 in 1X PBS for two hours. Primary rabbit polyclonal KCC3 antibody (1:200, [8]) was applied in the blocking buffer for 90 minutes at room temperature and transferred to 4°C overnight. The following day, fixed cells were washed with 1X PBS, for three consecutive washes, 10 min per wash. For secondary antibody, goat anti-rabbit IgG H&L (FITC) secondary antibody (1:200, Abcam, ab6717) was resuspended in blocking buffer and placed on the fixed cells for 2 hours at room temperature. Cells were then washed for three consecutive washes, 10 min per wash in 1X PBS and mounted with Prolong Gold antifade reagent with DAPI. The fixed cells were imaged on a Zeiss LSM 880 microscope. The same procedure was done for staining with the KCC2 antibody (1:200, Abcam, ab49917).

For staining, dorsal root ganglia were extracted as described above. They were then fixed in 10% formalin at room temperature, overnight. Once fixed, the tissue was embedded in paraffin and 10 micron thick sections were prepared. The paraffin was dissolved using Citrisolv (Thermo Fisher Scientific) and the tissue was rehydrated in 5 min consecutive washes of 100%, 95%, 70% ethanol, followed by a 10 min wash in 1X PBS. Antigen retrieval was performed on the slides using Citra Plus (BioGenex, Freemont, CA). Sections were then blocked with a buffer consisting of 5% bovine serum albumin, 1% goat serum, and 0.5% Triton X-100, for two hours. Sections were incubated with a rabbit polyclonal KCC3 antibody (1:200, [7]) at room temperature for 1.5 hours, and then placed overnight at 4°C. The primary antibody was then washed in 1X PBS for 10 minutes (3X), and subsequently placed in secondary FITC antibody (1:200, Abcam, ab97063) at room temperature for 2 hours. Tissues were then washed in 1X PBS, mounted with and mounted with ProLong Gold antifade reagent with DAPI (Life Technologies, Grant Island, NY), and imaged on a Zeiss LSM 880 microscope.

Data analysis and Statistics

Cell water volume was determined using the arbitrary fluorescent measurements from the NIS elements time-lapse tool to measure intensity. Cells were chosen based on whether they responded to the final osmotic challenge of returning to isotonic solution. Leak of calcein over time can cause fluorescent changes that are independent of cell volume. Therefore, the fluorescent signal from cells that appeared to have dye leakage was corrected as previously described [24]. GraphPad Prism8 was used for all statistical analysis.

All data are reported as means ± SEM. One-way ANOVA tests for generally followed by post-hoc Tukey tests to determine significance among specific groups.
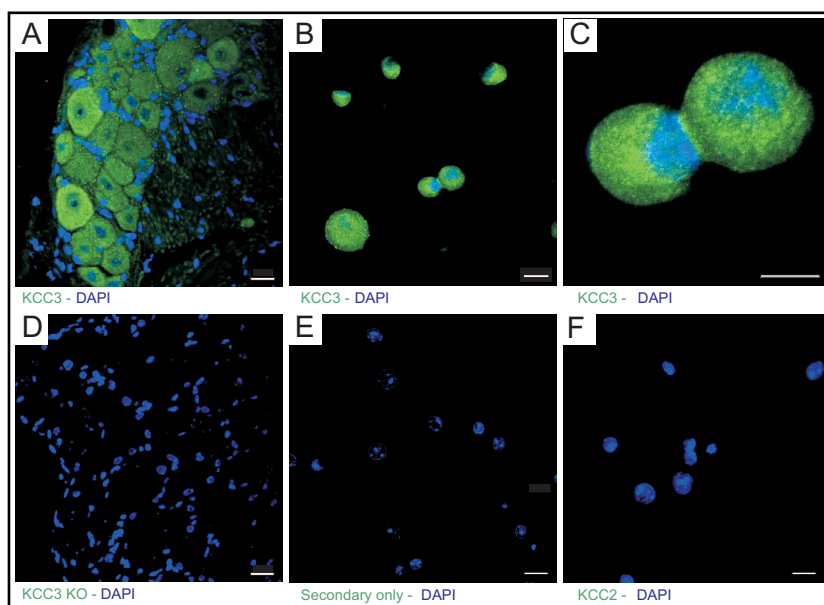
Results

Use of primary sensory neurons as a model for cell volume regulation

We utilized two available KCC3-targeted mouse lines to assess the role of KCC3 in cell volume regulation: a loss- of-function (LOF) line [1] and a gain-of-function (GOF) mouse line [16]. We compared these two lines to control littermates (mice with no mutations in KCC3) and also compared neurons from wild-type animals with neurons pharmacologically treated with the potent KCC2/KCC3 inhibitor, ML077 [25]. Careful preparation of primary neurons on coverslips was critical in creating consistent, standardized results. First, glass cover slips were prepared two days prior to plating with an overnight incubation in 1% polyethylen-amine (PEI), followed by an additional overnight incubation with laminin (50 μg/ml). DRG were then extracted and plated as described in the method section. KCC3 has been shown previously to be expressed in sensory neurons [1, 7, 26]. To confirm KCC3 expression in our isolated DRG neurons, we fixed the cells the day after plating and co-stained the neurons with anti-KCC3 antibody and DAPI and observed strong KCC3 signal (Fig. 1A-B). No signal was observed when the cells were exposed to secondary antibody alone (Fig. 1C). Importantly, we observed no expression of KCC2 (Fig. 1F), the central nervous system-specific K-Cl cotransporter.

DRG cell volume was determined through calcein fluorescence measurements

All volume measurement experiments were also performed one day after plating. Experimental set up included a 25 min incubation period with Calcein-AM (0.03 μM) in isotonic medium (300 mOsm), a baseline period under isosmotic solution, followed by an osmotic challenge. For our first set of experiments, we analyzed our data by placing the pinhole to different regions of the cell (Fig. 2). The data was highly variable as some pinholes

Fig. 1. Expression of KCC3 in mouse DRG neurons. A, Section of dorsal root ganglion isolated from wild-type mice stained with rabbit anti-KCC3 polyclonal antibody, followed by FITC-conjugated anti-rabbit antibody. B-C, DRG neurons isolated from wild-type mice stained with rabbit anti-KCC3 polyclonal antibody followed by FITC-conjugated anti-rabbit antibody. D, Section of dorsal root ganglion isolated from KCC3 knockout mice, stained with rabbit anti-KCC3 polyclonal antibody, followed by FITC-conjugated anti-rabbit antibody. E, Isolated dorsal root ganglion neurons stained with secondary antibody only. F, wild-type DRG neurons stained with rabbit anti-KCC2 polyclonal antibody show absence of KCC2 expression. All slides were mounted with DAPI-containing mounting reagent to stain nuclei. Bars: 20 μm for A, B, D-F and 10 μm for C.
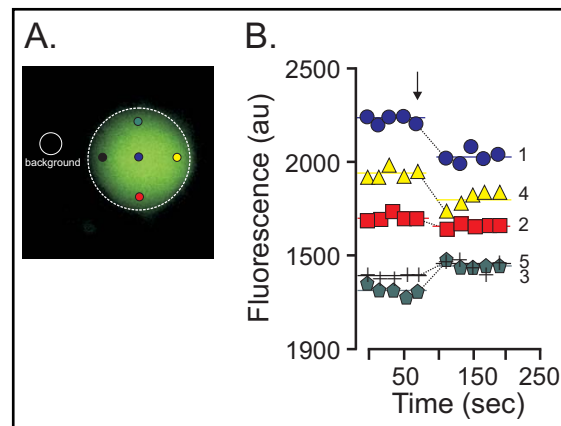
gave the typical decrease in fluorescence due to dye dilution during cell swelling, while others gave either no change or an increase in fluorescence signals. The data were, however, highly consistent when the pinholes were selected around the center of the cell (Fig. 3A). In all cases, a significant decrease in fluorescence signal was observed with a tight average and a small signal variation (Fig. 3B-C). The fluorescence signal traced well with the measured volume of the neurons, based on the area of the cell (Fig. 3D). Fig. 3E provides the typical response of a control DRG neuron when baseline fluorescence is recorded in isotonic solution for 3 min, followed by a 10 minute 40% hypotonic challenge, and a return to isotonic solution for 3 min. The cell swelled rapidly, followed by a period of regulatory volume decrease. When the cells are returned to isosmotic conditions, the volume overshoots as the cells have lost osmolytes. The perfusion bath system was designed in such a way that the open chamber refills with the new solution in a matter of seconds, allowing rapid changes in fluorescence (volume) to be detected. The

Fig. 2. Calcein fluorescence measurements in dorsal root ganglion neurons. A, Micrograph image taken on a widefield microscope, showing an isolated neuron loaded with calcein and background surrounding signal. Colored circles provide the position of the small "pinholes" that were used to acquire fluorescent signal during the swelling phase of the neuron during a hypotonic treatment. B, Hypotonic stress was applied at the three minute mark (arrow in figure), variability of signals with only blue and yellow pinholes showing anticipated decrease in fluorescence, whereas no fluorescence or even increased fluorescence were observed at the red and green pinholes, respectively.

extent of swelling (1), rate of swelling (slope, 2), rate of RVD (3), the rate of shrinkage upon return to isosmotic conditions (4), and the extent of overshoot (5), are all parameters measured in this type of experiment (Fig. 3E).

Neurons from wild-type (with or without KCC inhibitor), loss of KCC3 function, or gain of KCC3 function display different responses to the osmotic challenge

For this set of experiments, we isolated DRG neurons from 2-3 mice per genotype and recorded the response of a large number of neurons per preparation. All neurons were subjected to the 3 min isotonic baseline recording. At 3 min, the perfusion solutions were rapidly changed from isotonic to a 40% hypotonic osmotic shock and the cells were monitored for 10 minutes. The cells were then returned to isotonic media to assess the ability of the neurons to return to baseline. If a cell did not properly respond to the return under isosmotic solution, this cell was eliminated from further analysis.
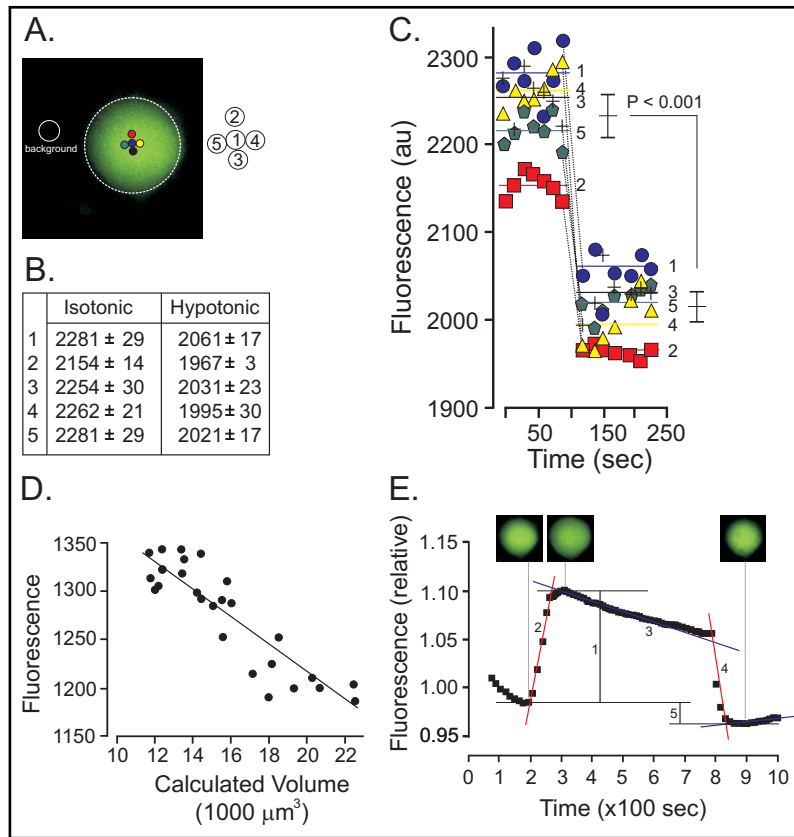
As neurons were exposed to hypotonic solution, they all swelled, but surprisingly to different degrees. Control neurons swelled by 11.5%, and with a rate of 0.0017 sec^{-1} (Fig. 4, 5A-B). Cells that lacked KCC3 increased their volume by 13.6% with a slower rate of 0.0008 sec^{-1}, whereas cells that express the constitutively active transporter demonstrated a blunted swelling response: 9%, and also with a slower rate of 0.0011 sec^{-1}. Finally, control neurons exposed to the KCC-specific ML077 inhibitor also showed an increased swelling over no inhibitor (although statistically not significant) with a rate of 0.0018 sec^{-1} (Fig. 4, 5A-B). The slopes amongst genotypes and treatment differed significantly ($P = 0.0001$). When the data were calculated by using time to half-peak rather than peak swelling, the data were similar (data not shown).

Following the swelling phase, most cells undergo regulatory volume decrease through a process that involves the loss of K$^+$ and Cl$^-$ ions, and obligatory water. Control DRG neurons exhibited such a behavior (Fig. 4, 5C). Interestingly, no regulatory volume decrease phase

Fig. 3. Calcein fluorescence measurements in dorsal root ganglion neurons. A, Micrograph showing an isolated neuron pre-loaded with calcein-AM and background surrounding signal. Several pinholes, indicated by colored circles, were positioned around the center of the neuron. B, Average fluorescence values obtained under isotonic (0 – 100 sec) and hypotonic (100 – 250 sec) conditions. C, same data presented in graph form with average fluorescence decreasing significantly upon cell swelling. D, Linear relationship between fluorescence signal and cell volume measured through the area of the neuron. E, Typical curve of fluorescence over time of neurons exposed to a hypotonic solution. The

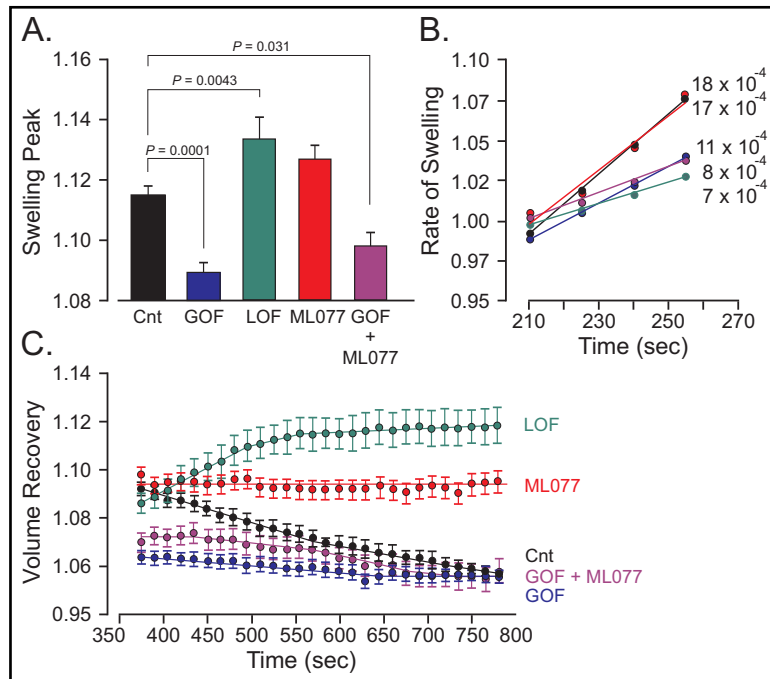|	Isotonic	Hypotonic
1	2281 ± 29	2061± 17
2	2154 ± 14	1967± 3
3	2254 ± 30	2031±23
4	2262 ± 21	1995±30
5	2281 ± 29	2021±17

graph can be divided into a swelling phase (extent of swelling: 1, and rate of swelling: 2), regulatory volume decrease phase (3), a shrinkage phase when the cells are returned to isosmotic conditions (4) and possible volume overshoot (5). Neuron insets show larger neuron at peak of swelling with decreased fluorescence.

Fig. 4. Osmotic behavior of neurons exposed to a hypotonic challenge. Neurons from wild-type (black), KCC3 knockout (or LOF, green), KCC3-T991A (or GOF, blue), and wild-type exposed to ML077 (red) were exposed to a 40% hypotonic shock. Fluorescence signals were averaged from 3 mice, 152 neurons for controls, 3 mice, 98 neurons for loss of function, 3 mice, 229 neurons for gain of function (T991A), and 3 mice, 134 neurons for the ML077 condition. FΔ/F0 is calculated as the change in fluoresce (intensity value during hypotonic response) divided by the averaged isotonic values. Values are means ± SEM.
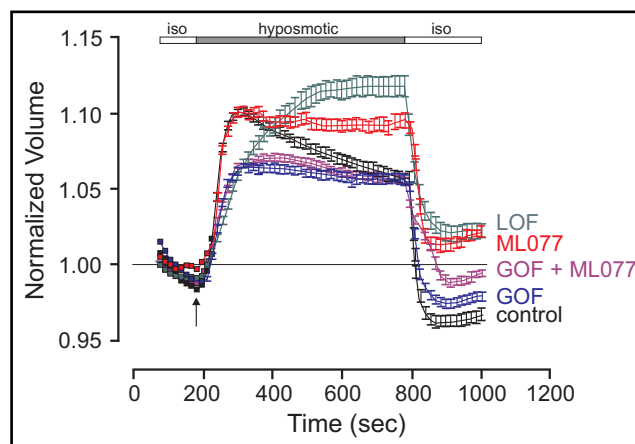

was observed in DRG neurons lacking KCC3 expression, expressing a constitutively active transporter, or exposed to the KCC-specific inhibitor, ML077. In fact, DRG neurons lacking KCC3 kept swelling for a few more minutes without reaching a true plateau. Statistical analysis confirmed that the slopes were significantly different between conditions (P = 0.001).

Cellular Physiology and Biochemistry

Cell Physiol Biochem 2020;54:577-590

DOI: 10.33594/000000241
Published online: 8 June 2020

© 2020 The Author(s). Published by
Cell Physiol Biochem Press GmbH&Co. KG

584

Flores et al.: KCC3 and Neuronal Volume

Fig. 5. Osmotic behavior broken-down by components. A, Extent of swelling of control neurons (black bar), KCC3 gain-of function (T991A) neurons (blue bar), KCC3 loss-of-function (knockout) neurons (green bar) and wild-type neurons exposed to 10 µM ML077 (red bar). Note the significant (One-way ANOVA) reduction in swelling elicited by the neurons expressing the constitutively active transporter and significantly increased swelling elicited by neurons lacking KCC3 expression. Treatment with ML077 showed no significant difference compared to control (P = 0.06). Bars represent means ± SEM (the number of neurons per genotype is listed in the legend of Fig. 4). B, Rate of swelling as calculated by the slope of volume increase. Control neurons: y = 0.0011 x + 0.7596; control neurons with ML077: y = 0.0010 x + 0.7984; neurons expressing KCC3 gain-of-function: y = 0.0007 x + 0.8448; and neurons lacking KCC3: y = 0.0006 x + 0.8178. C, Regulatory volume decrease phase as measured over a 10 min period with only untreated wild-type neurons showing a negative slope.

Fig. 6. Osmotic behavior of neurons broken-down by components. A, rate of shrinkage of neurons when they are returned to isosmotic saline following a 10 min exposure to hypotonicity. Note that the slopes are not very different amongst genotypes. B, Extend of cell shrinkage. The Y axis represents relative fluorescence where 1 represents the original fluorescence of the cells under isosmotic solution prior to the osmotic shock. A negative bar (as for control neurons and KCC3 T991A neurons) represents a volume overshoot, whereas a positive bar (as KCC3 knockout neurons and wild-type neurons treated with 10 µM ML077) represents a volume still larger than the original volume of the neurons. Bars represent means ± SEM (3 mice, 98-229 neurons). Significance was calculated using one-way ANOVA followed by Tukey Post-hoc analysis test.
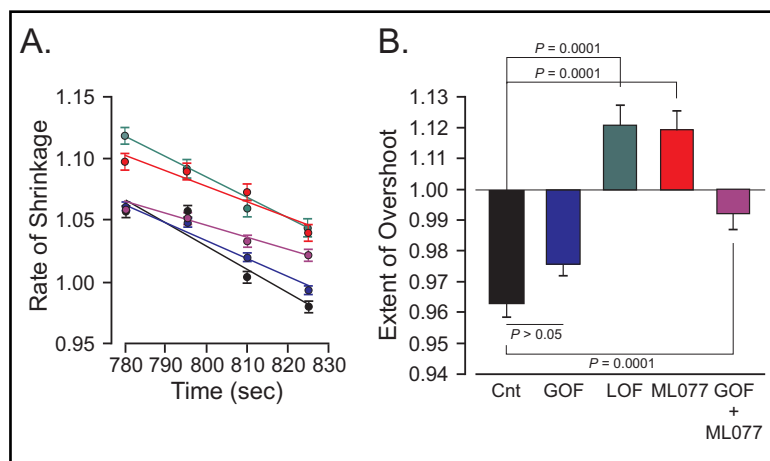
When the neurons were returned to isosmotic solution, they all shrunk. As seen in Fig. 6A, the slopes were not significantly different ($P = 0.05$). What was statistically significant was the position of the curves ($P = 0.0001$), which reflects the differences in swelling and RVD that the cells have experienced during the hypotonic phase. To determine the ability of

Fig. 7. Osmotic sensitivity of neurons. Van't Hoff plot showing fluorescence ratio versus osmotic pressure ratio of neurons exposed to 40% and 15% hypotonic and hypertonic shock. Note that the slope of the KCC3 gain-of-function neurons (blue dots and line, y = 0.126 x ± 0.8715) is lower than the slope of wild-type neurons (black dots and line, y = 0.1651 x ± 0.8330);

whereas the slope of the KCC3 knockout neurons (green dots and line, y = 0.1861 x ± 0.8211) is bigger that for wild-type neurons. (B) van't Hoff plot of neurons returning to isosmotic conditions. There was no significant difference among the slopes (P = 0.7) nor intercepts (P = 0.6). All slopes appear similar (control, y = 0.2563 x ± 0.7187; GOF y = 0.1984 ± 0.7742; LOF y= 0.2515 x ± 0.7419).
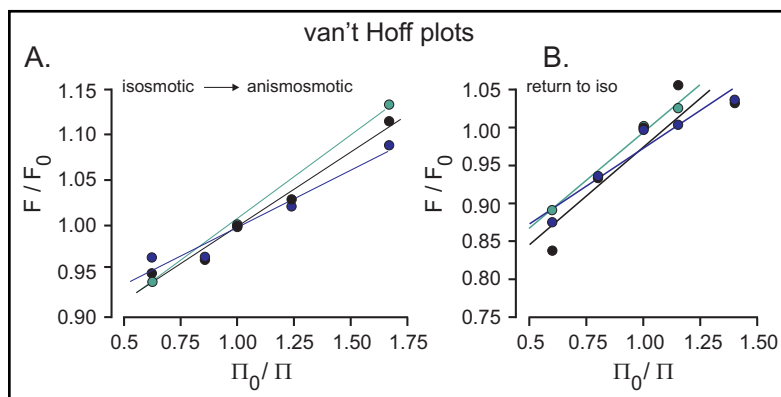
the DRG neurons to return their volume to baseline, we calculated the difference between the volume reached by the neurons following their return under isosmotic solution and the original volume of the cells. As seen in Fig. 6B, both control and constitutively active KCC3 neurons reached a new volume that was significantly lower than the original volume, whereas neurons lacking KCC3 expression (LOF) or function (ML077) did not fully return to their original volume. A one-way ANOVA showed an overall significant difference among means of osmotic recovery for all genotypes (P = 0.0001), with also significance at P = 0.0001 when comparing individually LOF with control neurons or ML077-treated neurons with control neurons. In contrast, there was no statistical difference between GOF and control (P = 0.05).

Osmotic behavior of DRG neurons: the van't Hoff plot

The osmotic phase of a cell depends primarily upon the water permeability of the membrane and the extent of the osmotic pressure imposed onto the cell. As we have seen in Fig. 4, the extent of swelling in response to a 40% osmotic shock was highly dependent on the genotype condition. To analyze further the osmotic behavior of the neurons, we exposed cells to milder hypotonic shock and to hypertonic shock and plotted the ratio of volumes versus ratio of osmotic pressures. The van't Hoff plots are depicted in Fig. 7A. It can be seen that the relationship of volumes versus pressures is linear over the range of applied pressure, but that the slopes differed significantly. Indeed, statistical analysis revealed a significant difference among the slopes (P = 0.04). Note that the van't Hoff slope of neurons expressing the constitutively active KCC3 transporter was significantly reduced compared to wild-type neurons, consistent with the reduced swelling of the LOF cells under the 40% hypotonic shock, whereas the slope of neurons lacking KCC3 expression is increased, again consistent with the increased swelling observed with these cells. We also produced van't Hoff plots for the volume changes observed when the cells are returned under isosmotic conditions after the original osmotic perturbation. As seen in Fig. 7B, there was no significant slope difference among the different groups of neurons (P = 0.7).

Discussion

We previously documented the first human case of a gain-of-function of KCC3 [16]. Similar to the patients with a loss of KCC3 function, this unique patient with the constitutive Thr991Ala mutation also exhibited sensorimotor neuropathy. In this case, however, there was no agenesis of corpus callosum or cognitive impairment. Experiments performed with

Cellular Physiology and Biochemistry

Cell Physiol Biochem 2020;54:577-590

DOI: 10.33594/000000241
Published online: 8 June 2020

© 2020 The Author(s). Published by
Cell Physiol Biochem Press GmbH&Co. KG

586

Flores et al.: KCC3 and Neuronal Volume

fibroblasts isolated from the patient surprisingly demonstrated an inability to swell upon hypoosmotic challenges, when compared to control fibroblasts [16]. Interestingly, analysis of nerve fibers from the KCC3-T991A mice revealed shrunken fibers [19]. Thus, it is clear that cell volume disturbance is a common feature in both KCC3 knockout and KCC3-constitutively active peripheral neurons and this implicates volume homeostasis as a critical factor for the health of peripheral nerve fibers.

The overarching goal of our experiments was two-fold. First, we wanted to assess the ability of sensory neurons from KCC3 wild-type, LOF and GOF mice to regulate their volume upon a hypotonic challenge. Second, we wanted to re-confirm with another native cell type, more relevant to the neuropathy, the unusual data that were observed with human fibroblasts expressing the overactive KCC3 transporter [16].

Overall, there were clear differences in the osmotic responses of GOF, LOF, and neurons treated with the KCC inhibitor ML077, when compared to control neurons. We assessed these difference by utilizing a fluorescent marker as a proxy for cell volume [22]. Our data confirm that using changes in the fluorescence signal of a dye was a reliable method to follow changes in cell volume as fluorescence signal has an inverse relationship with cell volume.

The swelling phase of cells during hypotonic treatment is typically regarded as strictly mediated by rapid water movement across the membrane to equilibrate the osmotic pressure. Cell membranes are indeed typically regarded as semi-permeable membranes, i.e. far more permeable to water than ions and other osmolytes. In fact, the estimated water permeability of biological membranes [27] ranges from 0.5 (as for water tight membranes, i.e. the bladder) – 40 (as for water permeable membranes, i.e. red blood cell) x 10^{-4} cm/s. Comparatively, the intrinsic ion permeability of a membrane to ions like Na^+ and K^+ is many orders of magnitude smaller (4-5 x 10^{-14} cm/s, [28]. As the water permeability of a membrane is only dependent on the lipid composition of this membrane and the presence or absence of water channels, one would assume that the water permeability of DRG neurons is identical amongst the different KCC3 genotypes and the cells would at least exhibit similar swelling behavior, even if they exhibit different volume regulation behaviors.

Indeed, control DRG neurons exposed to a 40% hypotonic shock exhibited the typical swelling phase, followed by a regulatory volume decrease phase. Although the cells did not return to their original volume over the 10 minute hypotonic shock, they clearly underwent regulatory volume decrease. The fact that the volume of these cells reached a volume smaller than the original volume when the cells were returned to isosmotic solution, confirmed that the RVD process was due to a loss of intracellular osmolytes. When control neurons were exposed to the KCC-specific inhibitor, they swelled to the same degree than wild-type cells, but did not volume regulate. The cells remained swollen for the duration of the hypotonic shock. This data indicates that the cotransporter is involved in the RVD process and may be responsible for the volume set point for activation of the cotransporter that exists under hypotonic conditions [29].

The behavior of the KCC3-knockout neurons and the KCC3-constitutively active neurons was surprising. As shown with fibroblasts isolated from the KCC3-T991A patient [16] and HEK293 cells transfected with a KCC3-T991A + T1048A mutant transporter [13], DRG neurons isolated from KCC3-T991A mice failed to properly swell under the 40% hypotonic shock. The extent of swelling was significantly reduced compared to wild-type cells.

The fact that DRG neurons isolated from KCC3-T991A mice did not swell to the same degree indicates that some of our assumptions are incorrect. First, we need to consider that the KCC3-T991A neurons already start with a smaller volume under isosmotic conditions. Indeed, on average, T991A neurons have a volume of approximately 10,000 μm^3 (N = 2 mice, n = 107 neurons) whereas control neurons are 10% larger with a baseline volume of 11,000 μm^3 (N = 1, n = 94). The mutant cells therefore have already a reduced amount of water and osmolytes. However, if they start with a smaller volume, and the swelling phase is purely osmotic, they should swell in the same proportion than wild-type cells.

Second, the explanation for the swelling discrepancy might be related to the assumption that the swelling is purely osmotic. It might possible that the constitutive activity of KCC3 al-

Cellular Physiology and Biochemistry

Cell Physiol Biochem 2020;54:577-590

DOI: 10.33594/000000241
Published online: 8 June 2020

© 2020 The Author(s). Published by
Cell Physiol Biochem Press GmbH&Co. KG

587

Flores et al.: KCC3 and Neuronal Volume

lows for a rapid loss of K^+ and Cl^- ions during the swelling phase, possibly large enough to reduce the extent of cell swelling. Unusually high ion permeability might indeed be possible as in human red blood cells, for instance, the Cl^- permeability is in the same order of magnitude than the water permeability of water-tight epithelia [28]. This high Cl^- permeability results from high expression levels of AE1, a Cl^-/HCO_3^- exchanger.

Note that in contrast to the T991A mutant cotransporter that would have a constitutively high K^+ and Cl^- permeability, the wild-type cotransporter needs a few minutes to activate when the cells are exposed to hypotonic stimuli. This lag phase, first described in red blood cells, was demonstrated to be due to swelling-induced inhibition of transporter phosphorylation, i.e. inhibition of a kinase [30]. Thus in wild-type cells, KCC3 would be silent during the swelling phase and allow for the full osmotic effect. The explanation of a rapid loss of ions, however, was rejected when DRG neurons isolated from KCC3-T991A mice were exposed to the 40% hypotonic shock in the presence of ML077. The inhibitor failed to restore the swelling extent to its original value.

Third, assumption that K-Cl cotransporters transport only K^+ and Cl^- ions was challenged by the work of Zeuthen who provided evidence for a direct KCC-mediated transport of water. He estimated a stoichiometry of about 500 water molecules for each K^+ and Cl^- ion [31]. Part of the evidence was that water movement could occur against an osmotic gradient. Whether this phenomenon is at play in KCC3-T991A neurons during their swelling phase is currently unknown. The recent cryo-EM structure of KCC1 [32, 33] does not provide any hint that direct water movement through the K-Cl cotransporter protein is possible.

As mentioned above, in their 2015 paper, Adragna and coworkers observed a similar reduction in swelling of fibroblasts transfected with constitutively active KCC3 [16]. They argued that NKCC1 in these conditions was activated as the extent of swelling could be restored by inhibiting the cotransporter with low doses of bumetanide. These data suggest that the transport of salt and water during the swelling phase is able to affect the extent of swelling. Indication that a rapid transport of ions and water during the swelling phase is supported by the demonstration that the intrinsic water permeability of the GOF neurons is, in fact, not different than control cells. Indeed, the rate of cell shrinkage when cells are returned to isosmotic conditions, as evidenced by the slopes (see Fig. 6A), was identical between genotypes.

When neurons isolated from KCC3 knockout mice were exposed to the 40% hypotonic shock, the cells swelled to a higher degree than wild-type cells (Fig. 4). This is also consistent with the idea that transport mechanisms can affect the swelling phase. However, the rate of swelling (slope to peak or to ½ peak) was reduced when compared to wild-type neurons, a phenomenon that we cannot fully explain. No RVD process was then observed in the KCC3 knockout neurons, consistent with the notion that loss of K^+ and Cl^- through the cotransporter mediates regulatory volume decrease in DRG neurons. These data also confirm previous data obtained with hippocampal pyramidal neurons and renal tubule proximal cells from KCC3 knockout mice versus wild-type mice. Both neurons and epithelial cells from knockout increased their volume to the same extent than wild-type cells, but the regulatory volume decrease phase was significantly blunted in the KCC3 knockout cells [6].

Another piece of evidence that KCC3 activity in wild-type neurons is involved in RVD comes from the overshoot observed when cells are returned to isosmotic conditions (Fig. 6B). The fact that the neurons shrank to a volume lower than the original volume indicates that the cells had lost osmolytes during their time under hypotonicity and the fact that neurons lacking KCC3 did not overshoot but instead showed a positive volume (Fig. 6B) confirmed the participation of KCC3 in the process. Interestingly, wild-type neurons exposed to ML077 during the hypotonic phase also failed to RVD and accordingly failed to overshoot when placed back under isotonic conditions. The fact that KCC3-T991A neurons exhibited a volume overshoot also implies that osmolytes were lost under the hypotonic phase. In this case, however, no RVD phase was observed, possibly indicating that the loss of ions/osmolytes instead occurred during the swelling phase.

In agreement with the lack of swelling of KCC3-T991A DRG neurons with a 40% hypotonic shock, the slope of the van't Hoff volume/osmolarity relationship was also significantly

Cellular Physiology and Biochemistry

Cell Physiol Biochem 2020;54:577-590

DOI: 10.33594/000000241
Published online: 8 June 2020

© 2020 The Author(s). Published by
Cell Physiol Biochem Press GmbH&Co. KG

588

Flores et al.: KCC3 and Neuronal Volume

reduced when compared to wild-type neurons. The fact that the volume versus osmolarity relationship is linear is in agreement with the osmotic behavior of most cells studied in the range of experimental osmolarities tested [34]. The reduced slope is indicative of a reduced ability of GOF neurons to swell under hypotonic conditions. The intercept of a typical van't Hoff plot on the Y axis provides the osmotically inactive volume, which in any cells ranges from 5-20%. The observation that the intercept of our van't Hoff lines in our experiments provides values of about 85% reflects the fact that a ratio of fluorescence is plotted as a proxy of volume. From the data of Fig. 3E, one can calculate that an 8% increase in fluorescence, in fact, corresponds to a 67% increase in cell volume. Thus, the intercept on the Y axis in our van't Hoff plots hardly represents the osmotically inactive volume.

The inability of KCC3 LOF neurons to volume regulate and inability of KCC3 GOF neurons to swell clearly indicate that these cells are unable to maintain volume homeostasis. This is in fact in full agreement with demonstration that nerve fibers from KCC3 knockout mice are swollen [7], whereas nerve fibers from KCC3-T991A mice are shrunken compared to the fibers of control littermates [19]. The inability of neurons to properly volume regulate likely accounts for the vacuolization and related pathology observed in the central nervous system [6] and peripheral nervous system [7, 8, 15]. The fact that a greater number of neurons (40% LOF and GOF versus 10% for controls) failed to "survive" the osmotic challenge (as evidenced by lack of shrinkage when returned under isosmoticity), validates the *in vivo* studies. Similarly, the number of DRG neurons that were isolated per mouse was significantly lower for KCC3 knockout mice, indicating the fragility of these neurons. It is likely that this inability to maintain volume integrity is at the basis of the nerve pathology and the inability of the nerve fibers to properly function. Ultimately, further work needs to be done to further understand the discrepancies we observe in cell swelling amongst mutations in KCC3, and how these disruptions ultimately lead to peripheral neuropathy in both humans and mice.

Acknowledgements

Disclosure Statement

The authors have no conflicts of interest to declare.

Cellular Physiology and Biochemistry

Cell Physiol Biochem 2020;54:577-590

DOI: 10.33594/000000241
Published online: 8 June 2020

© 2020 The Author(s). Published by
Cell Physiol Biochem Press GmbH&Co. KG

589

Flores et al.: KCC3 and Neuronal Volume

References

1   Howard H, Mount D, Rochefort D, Byun N, Dupré N, Lu J, et al.: The K-Cl cotransporter KCC3 is mutant in a severe peripheral neuropathy associated with agenesis of the corpus callosum. Nat Genet 2002;32:384–392.

2   Dupré N, Howard HC, Rouleau GA: Hereditary Motor and Sensory Neuropathy with Agenesis of the Corpus Callosum, in Adam M, Ardinger H, Pagon R (eds): GeneReviews® [Internet]. Seattle, University of Washington, Seattle, 2006.

3   Howard H, Dubé MP, Prévost C, Bouchard JP, Mathieu J, Rouleau G: Fine mapping the candidate region for peripheral neuropathy with or without agenesis of the corpus callosum in the French Canadian population. Eur J Hum Genet 2002;10:406–412.

4   Andermann F, Andermann E. Callosal Agenesis: A Natural Split Brain?, in Lassonde M, Jeeves M (eds): Advances in Behavioral Biology. Montreal, Springer, 1994, pp 19–26.

5   Mathieu J, Bedard F, Prevost C, Langevin P: Neuropathie Sensitivo-Motrice Hereditaire avec ou sans Agenesie du Corps Calleux: Etude Radiologique et Clinique de 64 Cas. J Neurol Sci 1990;17:103–108.

6   Boettger T, Rust M, Maier H, Seidenbecher T, Schweizer M, Keating D, et al.: Loss of K-Cl co-transporter KCC3 causes deafness, neurodegeneration and reduced seizure threshold. EMBO J 2003;22:5422–5434.

7   Byun N, Delpire E: Axonal and periaxonal swelling precede peripheral neurodegeneration in KCC3 knock-out mice. Neurobiol Dis 2007;28:39–51.

8   Ding J, Delpire E: Deletion of KCC3 in parvalbumin neurons leads to locomotor deficit in a conditional mouse model of peripheral neuropathy associated with agenesis of the corpus callosum. Behav Brain Res 2014;274:128–136.

9   Lauf P, Adragna N: K-Cl cotransport: Properties and molecular mechanism. Cell Physiol Biochem 2000;10:341–354.

10   Mount DB, Mercado A, Song L, Xu J, George AL, Delpire E, et al.: Cloning and characterization of KCC3 and KCC4, new members of the cation-chloride cotransporter gene family. J Biol Chem 1999;274:16355–16362.

11   Rinehart J, Maksimova Y, Tanis J, Stone K, Hodson C, Zhang J, et al.: Sites of Regulated Phosphorylation that Control K-Cl Cotransporter Activity. Cell 2009;138:525–536.

12   Lauf PK, Bauer J, Adragna N, Fujise H, Zade-Oppen M, Ryu KH, et al.: Erythrocyte K-Cl cotransport: Properties and regulation. Am J Physiol 1992;263:C917-C932.

13   Salin-Cantegrel A, Rivière JB, Dupré N, Charron FM, Shekarabi M, Karéméra L, et al.: Distal truncation of KCC3 in non-French Canadian HMSN/ACC families. Neurology 2007;69:1350–1355.

14   Shekarabi M, Moldrich R, Rasheed S, Salin-Cantegrel A, Laganière J, Rochefort D, et al.: Loss of Neuronal Potassium/Chloride Cotransporter 3 (KCC3) Is Responsible for the Degenerative Phenotype in a Conditional Mouse Model of Hereditary Motor and Sensory Neuropathy Associated with Agenesis of the Corpus Callosum. J Neurosci 2012;32:3865–3876.

15   Auer R, Laganière J, Robitaille Y, Richardson J, Dion P, Rouleau G, et al.: KCC3 axonopathy: neuropathological features in the central and peripheral nervous system. Mod Pathol 2016;29:962–976.

16   Kahle K, Flores B, Bharucha-Goebel D, Zhang J, Donkervoort S, Hegde M, et al.: Peripheral motor neuropathy is associated with defective kinase regulation of the KCC3 cotransporter. Sci Signal 2016;9:ra77.

17   De Los Heros P, Alessi D, Gourlay R, Campbell D, Deak M, Macartney T, et al.: The WNK-regulated SPAK/OSR1 kinases directly phosphorylate and inhibit the K^+-Cl^- co-transporters. Biochem J 2014;458:559–573.

18   Adragna N, Ravilla N, Lauf P, Begum G, Khanna A, Sun D, et al.: Regulated phosphorylation of the K-Cl co-transporter KCC3 is a molecular switch of intracellular potassium content and cell volume homeostasis. Front Cell Neurosci 2015;9:255.

19   Flores B, Schornak C, Delpire E: A role for KCC3 in maintaining cell volume of peripheral nerve fibers. Neurochem Int 2019;123:114–124.

20   Sleigh JN, Weir GA, Schiavo G: A simple, step-by-step dissection protocol for the rapid isolation of mouse dorsal root ganglia. BMC Res Notes 2016;9:82.

21   Alvarez-Leefmans F, Herrera-Pérez J, Márquez M, Blanco V: Simultaneous measurement of water volume and pH in single cells using BCECF and fluorescence imaging microscopy. Biophys J 2006;90:608–618.

22   Altamirano J, Brodwick M, Alvarez-Leefmans F: Regulatory volume decrease and intracellular Ca^{2+} in murine neuroblastoma cells studied with fluorescent probes. J Gen Physiol 1998;112:145–160.

23   Crowe W, Altamirano J, Huerto L, Xochimilco C, Alvarez-Leefmans FJ: Volume Changes in Single N1E-115 Neuroblastoma cells measured with a fluorescent probe. Neuroscience 1995;69:283–296.

24   Muallem S, Zhang B, Loessberg P, Starr A: Simultaneous Recording of Cell Volume Changes and Intracellular pH or Ca^{2+} Concentration in Single Osteosarcoma Cells UMR-106-01. Mol Biol 1992;267:17658–17664.

25   Delpire E, Days E, Lewis LM, Mi D, Kim K, Lindsley CW, et al.: Small-molecule screen identifies inhibitors of the neuronal K-Cl cotransporter KCC2. Proc Natl Acad Sci U S A 2009;106:5383–5388.

26   Pearson M, Lu J, Mount D, Delpire E: Localization of the K^+–Cl^- cotransporter, KCC3, in the central and peripheral nervous systems: expression in the choroid plexus, large neurons and white matter tracts. Neuroscience 2001;103:481–491.

27   Stein W, Litman T. Channels, Carriers, and Pumps: An Introduction to Membrane Transport. San Diego, Academic Press, 1990.

28   Hauser H, Phillips MC, Stubbs M: Ion Permeability of Phospholipid Bilayers. Nature 1972;239:342–344.

29   Hoffmann E, Lambert I, Pedersen S. Physiology of cell volume regulation in vertebrates. Physiol Rev 2009;89:193–277.

30   Jennings M, Al-Rohil N: Kinetics of activation and inactivation of swelling-stimulated K^+/Cl^- transport: The volume-sensitive parameter is the rate constant for inactivation. J Gen Physiol 1990;95:1021–1040.

31   Zeuthen T: Cotransport of K^+, Cl^- and H_2O by membrane proteins from choroid plexus epithelium of Necturus maculosus. J Physiol 1994;478:203–219.

32   Liu S, Chang S, Han B, Xu L, Zhang M, Zhao C, et al.: Cryo-EM structures of the human cation-chloride cotransporter KCC1. Science 2019;366:505–508.

33   Delpire E, Guo J: The cryo-EM structures of DrNKCC1 and hKCC1: a new milestone in the physiology of cation-chloride cotransporters. Am J Physiol Cell Physiol 2020;318:C225-C237.

34   Delpire E, Gagnon KB: Water Homeostasis and Cell Volume Maintenance and Regulation. Curr Top Membr 2018;81:3-52.